

ENHANCED DETECTION IN RESONANT SENSORS USING A SELF-TUNED SUPERCRITICAL HOPF BIFURCATION

Author: J. Tapson

Abstract

Self-tuned equilibrium at a supercritical Hopf bifurcation has been proposed as a mechanism for the high sensitivity and wide dynamic range of biological sensory systems. We present a simple circuit topology which demonstrates this dynamical behaviour. The topology includes a resonant element such as is present in many sensor and detector circuits, and has a single tuning parameter which varies the equilibrium point. Experimental results indicate an improved performance in detecting small and subthreshold signals, and no reduction in performance for large signals.

Introduction

It has been proposed that many biological sensory systems make use of local feedback loops to enhance their sensitivity [1,2]. Perhaps the best known case is the cochlea, in which inner hair cells act as sensors, and the outer hair cells and tip links may be modulated as feedback actuators to increase the detection sensitivity of the inner hair cells [3,4]. It has been demonstrated that this system may operate in equilibrium at a supercritical Hopf bifurcation [1,2,5]. Specifically, it is proposed that at low signal levels, the system is held on the threshold of limit cycling, and that subthreshold signals trigger and entrain these limit cycles, thereby increasing the signal to noise ratio (SNR) at the limit of detection.

In this paper we demonstrate a simple circuit, inspired by sensory models, which displays this dynamical behaviour. The sensing element of the circuit is a resonator, such as is used in many different types of sensor, as well as models of cochlear transduction [5]. We describe a system using a series resonant LCR circuit, although we have also successfully constructed the circuit with an electromechanical (piezoelectric) resonant element.

There are a number of well-known mechanisms, such as dithering and stochastic resonance [6,7], which act to increase SNR through the addition of extra energy to the

signal. The present system differs in that the nonlinearity is adaptively tuned in both amplitude and frequency, in order to best discriminate the signal. This is an inherent property of the new topology. In the extreme, at high signal amplitudes, the nonlinearity is completely eliminated from the signal path.

The enhancement of detection by emergent oscillatory behavior in sensors has been shown recently by Bulsara and co-workers in systems of coupled bistable magnetic elements [8,9]. To the best of our knowledge, this has not been demonstrated in simple resonant sensor circuits, although the use of feedback-induced instability is of course fundamental in most simple oscillators. Most recently, the equivalence of the Barkhausen criterion for linear oscillators and the conditions for Hopf bifurcation in nonlinear limit-cycling systems has been highlighted [10], so the existence of a supercritical Hopf bifurcation, and the onset of oscillation with the emergence of a high-gain nonlinear feedback path, is consistent with both linear and nonlinear oscillator theory.

The use of arrays of coupled Hopf bifurcation circuits in silicon cochlea systems has also been examined by Stoop, Kern, and co-workers [5,11], who conclude that these circuits do in fact provide the nonlinearities which enable many well-known psychoacoustic effects.

Circuit Description

The circuit consists of a resonant element which filters (and, in some cases, would transduce) the input signal. The filtered signal is amplified in the usual way to produce a sensor output signal. The output signal is fed to a zero-crossing comparator, which produces a saturating signal indicating the polarity of the input. The output signal is also fed to an RMS to DC converter, which measures the power in the output signal. This power level is subtracted from a setpoint (desired) power level, and the error signal is used to control a resistive divider, implemented with a field effect transistor (FET), which adds a small proportion of the comparator output to the input signal.

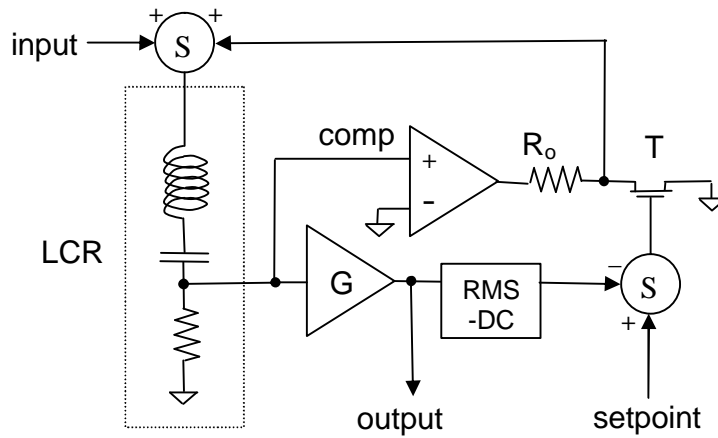


Figure 1: Block diagram of the system, with an *LCR* circuit as the resonant element. *G* indicates an amplifier and *comp* a comparator; *T* is a FET used in both linear and saturated regions. The RMS to DC converter produces a short-time average of the received signal strength, which modulates the level of feedback to the resonant circuit. Note that R_o should be large enough that when *T* is in saturation, their common node can be considered to be shorted to earth; i.e. the FET's channel resistance is negligible when driven in saturation, thereby shorting the feedback signal.

The system operates as follows: when the input signal is large enough to create a strong output signal, none of the comparator signal is fed back to the input, and the circuit is effectively a simple open-loop linear filter/transducer and amplifier. As the input signal amplitude is reduced, the feedback loop starts to inject some of the comparator signal back into the resonant element. If sufficient comparator signal is fed back, the circuit will act as a feedback oscillator and will start to limit cycle. However, if the feedback level is adjusted to be very low, the circuit can be kept on the threshold of limit cycling. The effect is then that the system is at the point of bifurcation (a supercritical Hopf bifurcation) [13], and the vestigial limit cycles will entrain with subthreshold signals and improve the resulting SNR.

The only tuning parameter in the circuit is the setpoint level of power (although the time constants in the RMS to DC conversion will affect the long-term system dynamics). In

practice, the power level would be set to give an output of the order of sensitivity of the detection system (e.g. of the order of the LSB amplitude of a downstream analog to digital converter). For coarse detection thresholds, this could require the system to operate well into the limit-cycling regime; whereas for very low thresholds the setpoint will be close to the noise floor.

Analysis

The circuit has two feedback paths. The bandwidths of operation of the two paths are separated by several orders of magnitude in frequency, so it is reasonable to model them independently. There is a fast second-order loop with a hard (step or “relay”) nonlinearity, and a slow first-order loop which controls the size of the step, and hence the limit cycle amplitude. If we make the reasonable approximation that the limit cycles are sinusoidal, the first order loop becomes linear, and we can use the describing function method [14] to analyze the second-order nonlinear loop. We can find a simple describing function for the limit cycles:

$$N(A, \omega) = \frac{4}{pA} (k - y_{rms}(t))$$

where A is the limit cycle amplitude, k is the rms setpoint, and $y_{rms}(t)$ is the actual rms value. Solving the characteristic equation for the nonlinear loop (using the describing function method) gives $A = 4(k - y_{rms}(t))/p$ and $\omega = 1/\nu(LC)$ as expected – the frequency is defined by the resonant circuit, and the amplitude of the limit cycles by the desired minimum signal strength. The stability of both loops is straightforward to demonstrate using standard frequency-domain methods such as the Nyquist criterion.

Performance

In analyzing small-signal response of phase-entraining circuits, there is a danger that measuring SNR simply in terms of power spectral density may give falsely optimistic results. (Consider for example the extreme case of a free-running phase-locked loop

which serendipitously matches the input signal.) We have measured the performance of this circuit using the coherence between input and output signals, defined as [14]:

$$g_{XY}^2(f) = \frac{|G_{XY}(f)|^2}{G_{XX}(f)G_{YY}(f)}$$

Where $G_{XY}(f)$ is defined in terms of the (single sided) cross-correlation function $R_{XY}(t)$:

$$G_{XY}(f) = 2 \int_{-\infty}^{\infty} R_{XY}(t) e^{-j2\pi ft} dt$$

Fig 2 shows coherence values for four cases. In two cases, the input signal is at the resonant frequency, and in the other two the input is at 90% and 110% of the resonant frequency. In the first case, the circuit is operating in open loop with the feedback disabled (i.e. as a simple linear detector); in the latter three cases the circuit is operating correctly in closed loop. For the off-resonance cases, the coherence values at the input frequencies are also shown. The Q of the resonant system was 10 and the detector gain was unity (in fact, no detector amplifier or buffer was used – a worst-case scenario).

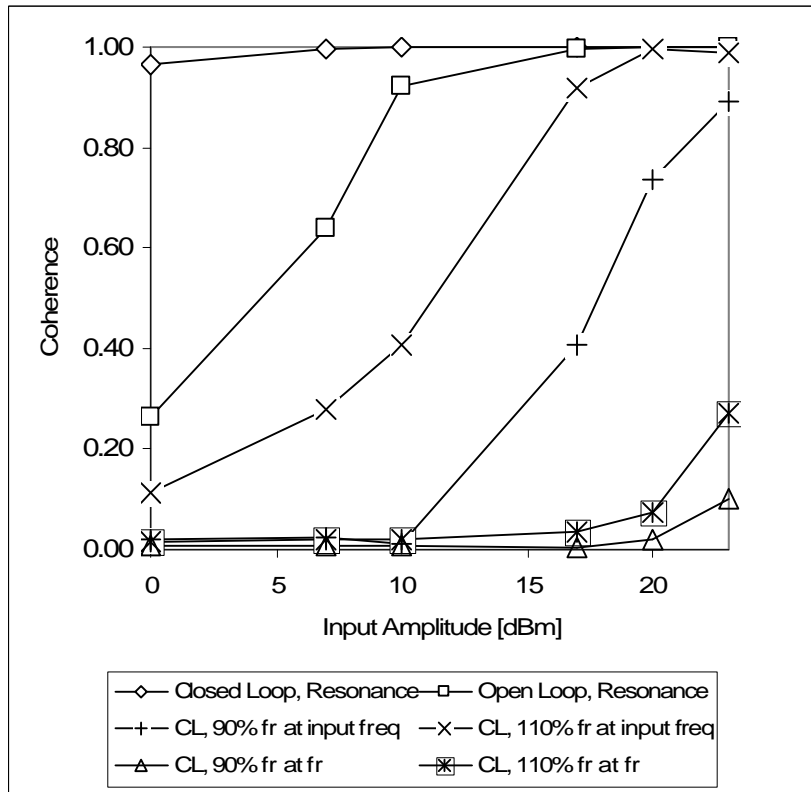


Figure 2: The coherence of input and output signals for several test cases. The uppermost curve (◇) represents the circuit detecting a signal at the resonant frequency. The coherence, even at 1dBm input, is 96%. By contrast, with the feedback disabled (□), the coherence drops to 26%. The lower four curves show closed-loop (CL) detection for input signals at $0.9 f_r$ and $1.1 f_r$, measured at the resonant frequency f_r (+ and ×) and also at the input frequency (△ and ⊠).

It can be seen that the small-signal detection is substantially improved by the detector – at the lowest signal input (1mV peak-peak), the coherence is 96%, compared with 26% for the linear case.

Conclusions

By introducing a tunable nonlinear feedback path, we have induced a self-tuning, stable supercriticality in a resonant detector circuit. As predicted by neurosensory researchers,

we have found that this improves the signal detection and frequency selectivity of the circuit. We believe this topology will find application in neuromorphic systems such as silicon cochleas, where this represents an improvement in both functionality and biological fidelity.

List of References

1. V. M. Eguíluz, M. Ospeck, Y. Choe, A. J. Hudspeth, and M. O. Magnasco, Essential Nonlinearities in Hearing, *Phys. Rev. Lett.* 84, 5232–5235 (2000).
2. S. Camalet, T. Duke, F. Jülicher and J. Prost, Auditory sensitivity provided by self-tuned critical oscillations of hair cells
3. T. Gold, Hearing. II. The physical basis of the action of the cochlea. *Proc R Soc Lond B: Biol Sci* 135: 492–498, 1948
4. Y. Choe, M.O. Magnasco, and A.J. Hudspeth, *Proc. Nat. Acad. Sci. USA* 95, 15231-15236.
5. A. Kern, and R. Stoop, Essential Role of Couplings between Hearing Nonlinearities, *Phys. Rev. Lett.* 91, 128101, 2003.
6. W.R. Bennet, Spectra of quantized signals, *Bell. Syst. Technol. J.* 27, 446-478, 1948.
7. K. Wiesenfeld and F. Moss, Stochastic resonance and the benefits of noise: from ice ages to crayfish and SQUIDS, *Nature* 373, 33-36, 1995.

8. A.R. Bulsara, V. In, A. Kho. P. Longhini, A. Palacios, W.-J. Rappel, J. Acebrón, S. Baglio and B. Ando, Emergent oscillations in unidirectional coupled overdamped bistable systems, *Phys. Rev. E* 70, 036103, 2004.
9. J.A. Acebrón, W.-J. Rappel, and A.R. Bulsara, Cooperative dynamics in a class of linear coupled two-dimensional oscillators, *Phys. Rev. E* 67, 016210, 2003.
10. T. Ueta and T. Kawakami. An aspect of oscillatory conditions in linear systems and Hopf bifurcations in nonlinear systems. *Proc. NDES2004*, Evora, Portugal, May 9-13 2004.
11. J.-J. van der Vyver, A. Kern, and R. Stoop, Active component implementation of a biomorphic Hopf cochlea, *Proc. European Conference on Circuit Theory and Design (3)* 285-288 (2003).
12. S.H. Strogatz, *Nonlinear Dynamics and Chaos*, Westview Press, Cambridge, 1994.
13. J.-J.E. Slotine and W. Li, *Applied Nonlinear Control*, Prentice-Hall, New Jersey, 1991.
14. J.S. Bendat and A.G. Piersol, *Engineering Applications of Correlation and Spectral Analysis*, John Wiley and Sons, New York, 1980.

Author Affiliation:

Department of Electrical Engineering
University of Cape Town
Rondebosch 7701
South Africa